ACS APPLIED MATERIALS & INTERFACES

Research Article

www.acsami.org

Doping Level of Boron-Doped Diamond Electrodes Controls the Grafting Density of Functional Groups for DNA Assays

Ľubomír Švorc,[†] Daliborka Jambrec,[‡] Marian Vojs,[§] Stefan Barwe,[‡] Jan Clausmeyer,[‡] Pavol Michniak,[§] Marián Marton,[§] and Wolfgang Schuhmann*[,‡]

[†]Institute of Analytical Chemistry, Faculty of Chemical and Food Technology, Slovak University of Technology in Bratislava, Radlinského 9, SK-812 37 Bratislava, Slovak Republic

[‡]Analytical Chemistry—Center for Electrochemical Sciences (CES), Ruhr−Universität Bochum, Universitätsstrasse 150, 44780 Bochum, Germany

[§]Institute of Electronics and Photonics, Faculty of Electrical Engineering and Information Technology, Slovak University of Technology in Bratislava, Ilkovičova 3, SK-812 19 Bratislava, Slovak Republic

Supporting Information

ABSTRACT: The impact of different doping levels of boron-doped diamond on the surface functionalization was investigated by means of electrochemical reduction of aryldiazonium salts. The grafting efficiency of 4-nitrophenyl groups increased with the boron levels (B/C ratio from 0 to 20 000 ppm). Controlled grafting of nitrophenyldiazonium was used to adjust the amount of immobilized single-stranded DNA strands at the surface and further on the hybridization yield in dependence on the boron doping level. The grafted nitro functions were electrochemically reduced to the amine moieties. Subsequent functionalization with a succinic acid introduced carboxyl groups for subsequent binding of an amino-terminated DNA probe. DNA hybridization significantly depends on the probe density which is in turn dependent on the boron doping level. The proposed approach opens new insights for the design and control of doped diamond surface functionalization for the construction of DNA hybridization assays.

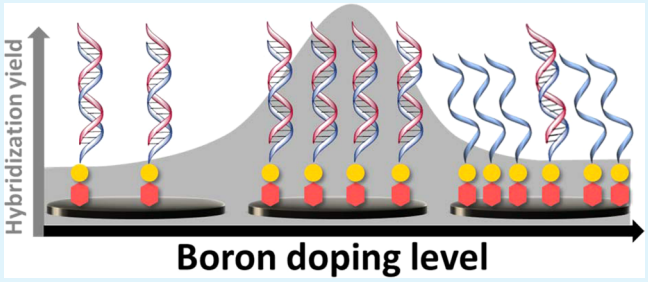

KEYWORDS: *boron-doped diamond, surface functionalization, electrochemical grafting, diazonium cations, DNA hybridization*

1. INTRODUCTION

Surface functionalization of various materials by covalent attachment of biologically active molecules has gained considerable attention in the past decade, aimed at developing biosensors or biointerfaces. Platform materials for these applications should possess several key properties: (i) bioinertness and biocompatibility, (ii) amenability for tailoring of its surface hydrophobicity, and (iii) suitable surface termination allowing for a robust attachment of a wide range of biomolecules.[1] Moreover, high oxygen and hydrogen evolution overpotentials are necessary to enable the reversible modification of surface reactivity without the destruction of the biosensors.[2] Various materials have been used for surface functionalization, such as metal oxides,[3] graphite,[4] glassy carbon,[5] gold,[6] polymers,[7] silicon,[8] etc. The primary drawbacks of most of these materials are long-term instability, low reproducibility, and inhomogeneity of related biointerfaces.[9] Hence, strategies for surface functionalization using controllable immobilization chemistries are still of utmost importance for the covalent attachment of active functional groups.

Conductive diamond films have emerged as an ideal platform material for biosensors and biointerfaces.[10] Their exceptional hardness, high chemical stability, excellent mechanical properties as well as inherent bioinertness and biocompatibility make them a favorable alternative to established materials.[2] In particular, boron-doped diamond (BDD) has received growing interest owing to its superior electrochemical properties such as large working potential window in aqueous solutions, low and stable background current, and negligible surface fouling.[11] These properties, in combination with its versatility, make BDD a material of choice for interfacing biomolecular entities. However, the electronic properties of BDD electrodes are dependent on a range of factors such as dopant concentration, structural defects in the diamond film, surface termination, nondiamond carbon impurity content (e.g., sp^2 inclusions), crystallographic orientation, and fraction of grain boundaries.[12] The chemical inertness of as-grown (hydrogen-terminated) BDD films prevents the direct biomolecule immobilization at the surfaces. Hence, BDD surface functionalization is required to provide suitable reactive groups (e.g., amino, thiol, or carboxylic acid groups) for subsequent covalent attachment of biomolecules. Accordingly, some efforts have been made to

Received: December 23, 2014
Accepted: August 18, 2015
Published: August 18, 2015

DOI: 10.1021/acsami.5b06394
ACS Appl. Mater. Interfaces 2015, 7, 18949−18956

functionalize BDD using either thermal[13] or chemical[14] surface activation as well as photochemical derivatization.[15] The possibility to use the thiol−yne reaction for linking thiolated molecules on alkynyl-terminated BDD surfaces in a controlled manner was recently investigated. This reaction allows for controlling the density of the linked molecules by adjusting the initial concentration of the thiolated molecules.[16]

Electrochemical functionalization using diazonium salts has been proved to be an efficient approach since it provides versatile functionality, high stability, and good flexibility concerning the tethered substituents.[17−20] Even though the grafting process is intrinsically challenging to control because of its radical nature, the degree of surface functionalization can be controlled by varying the grafting time and potential, the modifier concentration, the nature of the modifiers, and the intrinsic properties of the substrate surface itself. This methodology has been applied to doped diamond surfaces for grafting of various entities such as enzymes,[21] proteins,[22] metal complexes,[23] or DNA.[24]

Surface termination and the doping level of diamond films affect the electronic properties (energy barriers) and depletion layer width at the solid/electrolyte interface, respectively.[2] By tuning these parameters, the efficiency of surface functionalization of diamond electrodes can be effectively controlled. Even though there have been some reports directed to the effect of hydrogen and oxygen termination on electrochemical grafting of aryldiazonium salts,[25−27] no systematic studies exploring the effect of boron doping levels on the grafting and related biomolecule sensing efficiency have been made until now.

We introduce here a strategy for tuning of the surface functionalization of BDD electrodes based on the variation of their boron doping level. We investigated the effect of the boron doping level on the electrochemical grafting of aryldiazonium salts, the related density of immobilized single-stranded DNA capture probes, and the influence on the yield of complementary DNA hybridization.

2. EXPERIMENTAL SECTION

2.1. Apparatus. Electrochemical measurements were performed in a single compartment glass cell using an AUTOLAB PGSTAT 302N (Metrohm Autolab, The Netherlands) potentiostat controlled by the NOVA 1.10 software. A standard three-electrode system was used employing a Ag/AgCl/3 M KCl as reference electrode (all potentials are quoted relative to this reference) and a Pt wire as auxiliary electrode. Bare BDD (with a geometric area of 0.43 mm^2, preparation in Section 2.3) and modified BDD electrodes with different boron doping levels were used as working electrodes. These measurements were performed at room temperature. The morphology and structure of the BDD electrodes were characterized by scanning electron microscopy (SEM, JEOL JSM-7500F) and Raman spectroscopy (HORIBA JOBIN YVON LABRAM 300, He−Ne laser 633 and/or 325 nm). To determine the boron doping level in diamond in relation to the B/C ratio in the gas phase during the deposition process, Hall constant measurements, Raman spectroscopy, neutron depth profiling (NDP), and secondary ion mass spectroscopy (SIMS) were carried out. NDP was used utilizing a strong nuclear reaction of $^{10}B(n, \alpha)^7Li$ with a high cross section (3837 b) with the detection limit of 10^{12} B atoms per cm^3 and 15 nm as the depth resolution of the technique. SIMS was done by an Ion-TOF SIMS IV instrument with a high energy Bi^+ primary source combined with low energy sputtering gun (Cs^+). The boron concentration conversion was done using the RSF value of 10^{24} cm^{-3}. The method for obtaining the boron concentration from Hall constant measurement is described elsewhere.[28]

2.2. Chemicals. 4-Nitrophenyldiazonium tetrafluoroborate was prepared as explained in the Supporting Information (SI). Sulfuric acid (VWR, Darmstadt, Germany), potassium chloride (Mallinckrodt Baker, The Netherlands), and phosphate buffer were used as electrolytes. Phosphate buffer (PB, pH 7.4) was prepared by mixing stock solutions of potassium hydrogen and dihydrogen phosphates with adjustment of potassium sulfate (all purchased from VWR, Darmstadt, Germany). Succinic acid and 1,1′-carbonyldiimidazole (CDI) were from Sigma-Aldrich (Steinheim, Germany) and used without further purification. Potassium hexacyanoferrate(II) trihydrate and potassium hexacyanoferrate(III) were obtained from Sigma-Aldrich (Steinheim, Germany). All reagents were of analytical grade and used as received. Ultrapure water (>18 MΩ cm) was used to prepare all solutions.

DNA oligonucleotides with an *Escherichia coli* E447 strain sequence complementary to a hypervariable region of S16 RNA were purchased from FRIZ Biochem (Neuried, Germany). The sequences of the immobilized single-stranded DNA (NH_2-ssDNA; S1) capture probe was 5′-GTCAATGAGCAAAGGTATTAACTTTACTCCCTTCC-TCCTTTTTTTTNH_2 (C6) and the ferrocene-labeled target DNA strand (S2, fully complementary to S1) was 5′-$(Fc)_4$GGAGGAAGG-GAGTAAAGTTAATACCTTTGCTCATTGAC). The oligonucleotides were dissolved in PB (pH 7.4) and kept frozen.

2.3. Preparation of BDD Electrodes. Doped polycrystalline BDD films with various boron concentrations were grown by double bias enhanced hot filament chemical vapor deposition (HF CVD) as previously described.[29] As substrate, highly conductive (0.008−0.024 Ω cm) N (100) type silicon with a 2 μm thick SiO_2 layer (CVD, Oxford PlasmaLab 80) were used. The deposition process was divided into three steps: (i) 40 min ultrasonic seeding of diamond nanoparticles (CAS No. 7782-40-3, Sigma-Aldrich) diluted in deionized water, (ii) 2 h growth of the BDD thin film with 1% concentration of CH_4 in H_2 and trimethylborane (TMB) to obtain a 0 to 20 000 ppm boron to carbon ratio (B/C) in the gas mixture. The total pressure in the reactor was kept at 3000 Pa, and the temperature was set to 650 ± 20 °C, (iii) a hydrogen termination of the as-grown BDD layer within one vacuum cycle (10 min, H_2, 3000 Pa, 650 ± 20 °C). The resistivity of the films was 4×10^{-1} to 1.5×10^{-3} Ωcm, and the bulk concentration of charge carriers were 2.5×10^{19} to 3.7×10^{21} cm^{-3}, as measured by 4-point hall measurements.[28] The active surface area (0.43 mm^2) of the working electrode was created in 400 nm SiO_2 (CVD, Oxford PlasmaLab 80) by using standard optical lithography (SUSS, MA6) and wet etching in BOE solution (6:1 volume ratio of 40% NH_4F in water to 49% HF in water). Subsequently, the electrode chip (10 × 3 mm^2) was electrically connected by an Ag polymer paste (CB115, DuPont) to a printed circuit board support and subsequently completely passivated by a nonconducting paste (548X, DuPont).

2.4. Measurement Procedures. Prior to use, the bare or modified BDD electrodes were sequentially pretreated by thorough rinsing with ultrapure water, 5 min soak in methanol, followed by another thorough rinsing with ultrapure water, and finally blown dry using argon gas. Afterward, electrochemical cleaning of bare BDD electrodes was performed by applying +2.5 V for 180 s in 0.5 M H_2SO_4. Following this step, the BDD electrodes were cathodically pretreated by applying −2.5 V for 180 s. All electrochemical experiments were carried out after deaeration of the solution by purging with argon gas for at least 15 min. Electrochemical grafting of the aryldiazonium salt and the following conversion of the nitro groups were investigated using cyclic voltammetry (CV). CV was additionally used to evaluate the electrochemical blocking properties after electrode functionalization using ferrocyanide/ferricyanide as freely diffusing redox couple. Differential pulse voltammetry (DPV) with a pulse height of 50 mV, pulse time of 50 ms, and a scan rate of 10 mV/s was employed for investigating DNA hybridization efficiency.

2.5. BDD Surface Functionalization. For electrochemical grafting of 4-nitrophenyl groups, CV in a potential range from +0.6 to −0.8 V (5 cycles, 200 mV/s) in 1 mM 4-nitrophenyldiazonium tetrafluoroborate (in 0.1 M H_2SO_4) was performed. The electrodes were then immersed into 0.1 M KCl solution for electrochemical reduction of the 4-nitrophenyl moiety to 4-aminophenyl groups using CV in a potential range between +0.2 and −1.5 V (5 cycles, 50 mV/s). Subsequently, the 4-aminophenyl modified electrodes were incubated

DOI: 10.1021/acsami.5b06394
ACS Appl. Mater. Interfaces 2015, 7, 18949−18956

Scheme 1. Preparation of Different Surface Functionalized BDD Electrodes with Various Boron Doping Levels for Assessment of DNA Hybridization Efficiency[a]

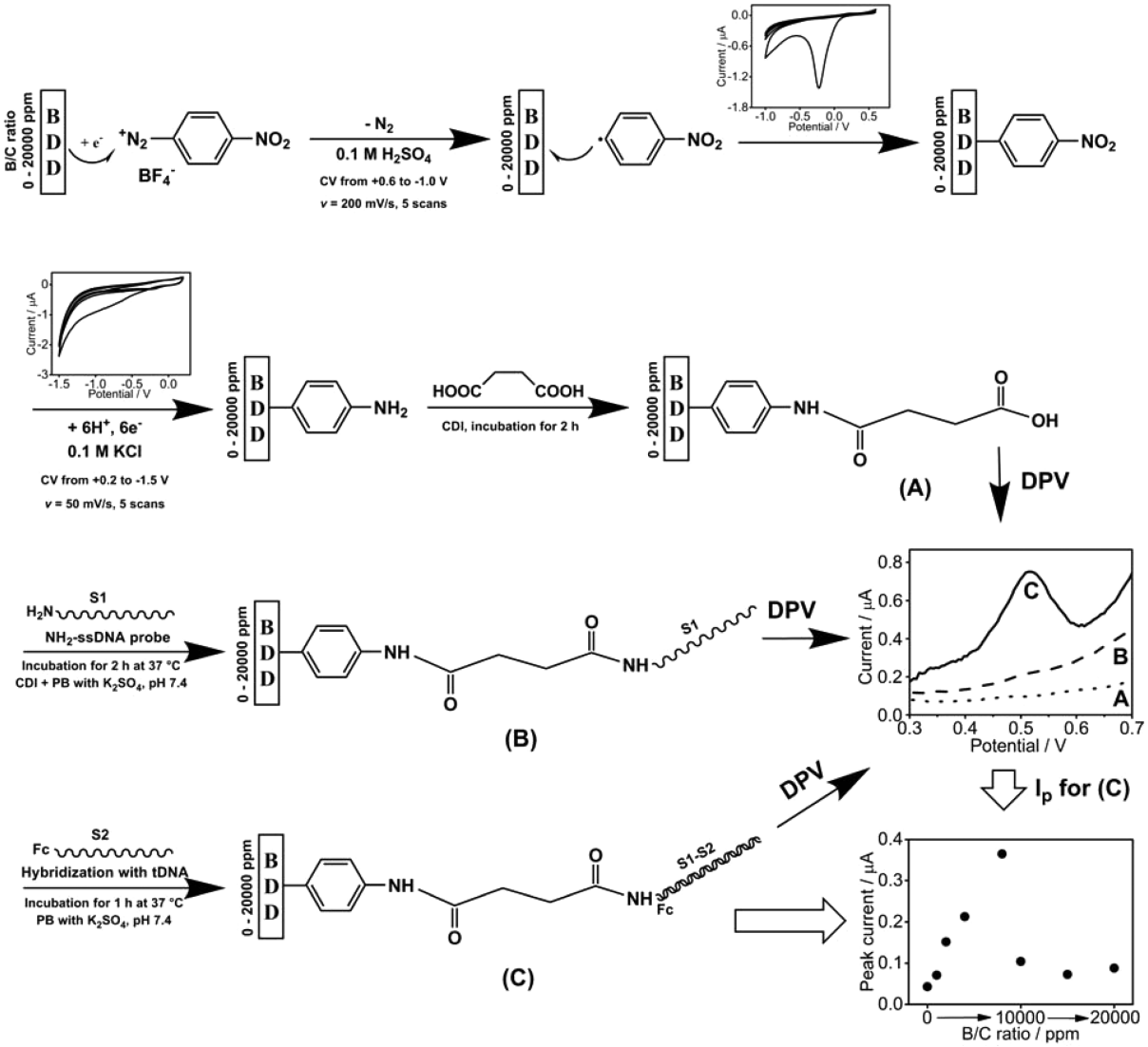

[a](A) COOH-BDD electrodes; (B) DNA probe modified BDD electrodes (S1/COOH-BDD); and (C) double stranded DNA (with Fc label) modified BDD electrodes (S1−S2/COOH-BDD).

in a solution of 0.1 M succinic acid containing 1,1′-carbonyldiimidazole (CDI, 1 mM) as activator for 2 h at room temperature to form activated carboxyl-modified BDD electrodes.

2.6. DNA Immobilization and Hybridization. For the immobilization of the single-stranded DNA probe (S1), the activated carboxyl-modified BDD electrodes were immersed in 10 mM PB (pH 7.4) containing 450 mM K_2SO_4 and 1 μM DNA probe and kept in a thermo-mixer (HTC BioTech, Ditabis, Germany) for 2 h at 37 °C. Subsequently, the electrodes were rinsed with the same buffer solution (excluding DNA) to remove nonspecifically bound DNA to obtain the S1 modified electrodes (S1/COOH-BDD). For hybridization S1/COOH-BDD electrodes were incubated in the same buffer solution containing 1 μM target ferrocene-labeled DNA (S2) for 1 h at 37 °C. Afterward, the electrodes were rinsed with buffer solution (S1−S2/COOH-BDD).

3. RESULTS AND DISCUSSION

3.1. Morphological and Structural Characterization of BDD Films. All prepared boron-doped diamond films on Si/SiO_2 substrates (BDD) show the typical polycrystalline structure with submicron crystal size. The difference in morphology is very small irrespective of the boron doping level. With increasing boron concentration, the average crystal size increases from approximately 200 to 500 nm (Figure S1). The thickness of the films varies from 283 nm for the film deposited without trimethylborane in the gas mixture to up to 502 nm for the highest B/C ratio. Selected properties of the deposited BDD films with boron concentration values in relation to the B/C ratio in the gas phase determined by Raman spectroscopy, Hall constant measurements, NDP, as well as SIMS are summarized in Table S1 and Figure S2, respectively. The boron concentrations were obtained from Raman spectra by deconvolution of the "500 cm^{-1}" maximum. Following the study of Bernard et al.,[30] we have fitted the band by one Lorentzian and one Gaussian line, while the position Lorentzian was used to calculate the boron concentration. Due to the strong Si maximum at 521 cm^{-1}, the boron concentrations were determined only for 4000 ppm and higher doped films.

DOI: 10.1021/acsami.5b06394
ACS Appl. Mater. Interfaces 2015, 7, 18949−18956

Raman spectra obtained using 633 nm laser excitation (Figure S3) exhibit the characteristic bands of BDD films. The boron doping is represented by two broad bands at approximately 500 and 1220 cm^{-1}, which are associated with the incorporation of boron into the diamond lattice.[29] The increase in its intensity follows the increase in the B/C ratio. As the boron concentration in the gas mixture increases, the peaks become more visible, and they finally dominate the Raman spectra for the highest boron concentrations. The maximum at 500 cm^{-1} is attributed to local vibrational modes of the boron pairs,[31] and the small shoulder at 1320 cm^{-1} is associated with polycrystalline diamond in highly boron-doped films. The peak at 1332 cm^{-1} corresponds to the sp^3 carbon phase in polycrystalline diamond. This peak was recorded in spectra of films with lower and no (residual) boron concentrations and was continually decreasing, broadening, and shifting to 1320 cm^{-1} with increasing boron level due to the so-called "Fano" effect. This phenomenon results from quantum interference between the "1332 cm^{-1}" zone center optical phonon and a continuum of electronic transitions at the same energy induced by the presence of the dopant.[32] The small bands at 1110 and 1430 cm^{-1} are associated with *trans*-polyacetylene at grain boundaries.[30] The sharp peak at 521 cm^{-1} and the broad one at 950 cm^{-1} belong to the Si. The change in its intensity is due to the changing thickness and transparency of the BDD films at different boron doping levels. It can also be seen in the Raman spectra (Figure S3), that the polycrystalline diamond films contain only a small amount of sp^2 carbon bonds. These are mainly located at grain boundaries, intra- or intergranular defects. Furthermore, owing to the missing D- and G- maxima in the spectra and inability to determine the amount of sp^2 (and sp^3) using 633 nm laser Raman spectra of BDD (because of the "Fano" effect, which makes both the sp^3 and sp^2 carbon bonds invisible with increasing B concentration), additional experiments were performed utilizing 325 nm laser excitation (Figure S4). These spectra are able to distinguish the increasing sp^2 content. By considering the I_D/I_G ratio obtained from the particular Raman spectra, we also have to take into account that the used UV laser is around 15−70 times more sensitive to sp^2 bonds than to sp^3 bonds. Assuming that the 325 nm Raman I_D/I_G ratio indicates continuous increase of sp^2 bond content from about 1.5% to 4% with the increase of the boron content in the gas phase during the deposition process of BDD films from 0 to 20 000 ppm. The percentage of sp^2 is usually inversely proportional to crystal size, as the surface of crystals (grain boundaries) is larger in the case of nanocrystalline diamond film than that for the microcrystalline one.[33] This low amount of sp^2 bonds, mainly located at the grain boundaries, will not have a crucial effect on the total amount of surface active sites of the electrodes. Especially when the used BDD films possess metal-like conductivity (except the 0 and 1000 ppm samples), the high conductivity and the resulting currents are mainly due to the B incorporation into the diamond lattice.

3.2. Electrochemical Grafting of 4-Nitrophenyl Groups. A general strategy for the preparation of surface functionalized BDD electrodes with different doping levels, and their further application is displayed in Scheme 1. Bare BDD working electrodes were first electrochemically hydrogenated using a procedure as described in Section 2.4. 4-Nitrophenyldiazonium tetrafluoroborate in 0.1 M H_2SO_4 was reduced at BDD electrodes by means of CV. Figure 1 displays the cathodic peaks in the first scan attributed to the electrochemical grafting of 4-nitrophenyl groups. In consecutive

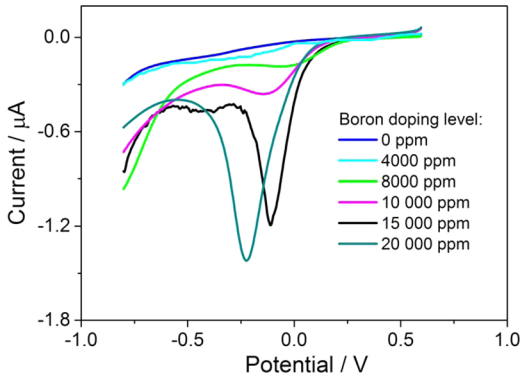

Figure 1. Cyclic voltammograms (first scan) of the electrochemical reduction of 1 mM 4-nitrophenyldiazonium tetrafluoroborate in 0.1 M H_2SO_4 at a scan rate of 200 mV/s for BDD electrodes with different boron doping levels.

scans, the reduction currents decrease remarkably due to the increasing surface passivation of BDD electrodes by additional 4-nitrophenylfunctionalities (not shown). This is in good agreement with previous studies at doped diamond and glassy carbon electrodes.[17,25,26] Therefore, it can be supposed that the generated 4-nitrophenyl radicals react with BDD surfaces under formation of C—C bonds.

The peak potentials of the diazonium cation reduction vary in a range from 0 to −0.25 V in dependence on the boron doping level. A low cathodic reduction potential is a characteristic of diazonium salts grafted at carbon electrodes.[20] However, when considering the peak currents and peak area, a substantial increase is observed with increasing boron doping level. Assuming equal Coulombic efficiency for all boron doping levels, the integration of the reduction peaks reveals that the grafting efficiency is 30-, 15-, and 6-fold higher for BDD electrode with a doping level of 20 000 ppm as compared to 0, 4000, and 10 000 ppm, respectively. The improvement of charge transfer with increasing boron doping level results in an improved attachment of 4-nitrophenyl moieties at the BDD electrode surface, as expected due to the increase in the specific conductivity.

To evaluate the electrochemical blocking properties of the grafted 4-nitrophenyl groups, CVs of BDD electrodes before and after grafting of 4-nitrophenyl groups were recorded in 5 mM $[Fe(CN)_6]^{3-/4-}$ in 0.1 M KCl. As shown in Figure 2 (black lines), BDD electrodes exhibit well-defined peaks with a significant improvement of the reversibility degree with the doping level. Furthermore, both cathodic (I_{pc}) and anodic (I_{pa}) peak currents increase with the doping level. This may be attributed to the increase of the density of electronic states formed within the band gap of doped diamond as the boron level increases. The reversibility parameters ΔE_p and I_{pa}/I_{pc} vary in the range of 1.62−0.15 V and 1.61−0.90, respectively, with considerable enhancement for diamond electrodes with a boron level higher than 4000 ppm ($\Delta E_p \approx 0.30-0.15$ V, $I_{pa}/I_{pc} \approx 1.22-0.90$). The properties of BDD electrodes with a high doping level are usually described as "metallic" suggesting direct electron transfer between the valence or conduction band of the electrode and the redox species in solution. However, the presence of more boron impurity centers may cause increased scattering in the diamond.[34] This is supposed to be responsible for the slight loss of the reversibility degree and the decrease of peak currents in the case of the BDD electrode with a doping level of 20 000 ppm.

DOI: 10.1021/acsami.5b06394
ACS Appl. Mater. Interfaces 2015, 7, 18949−18956

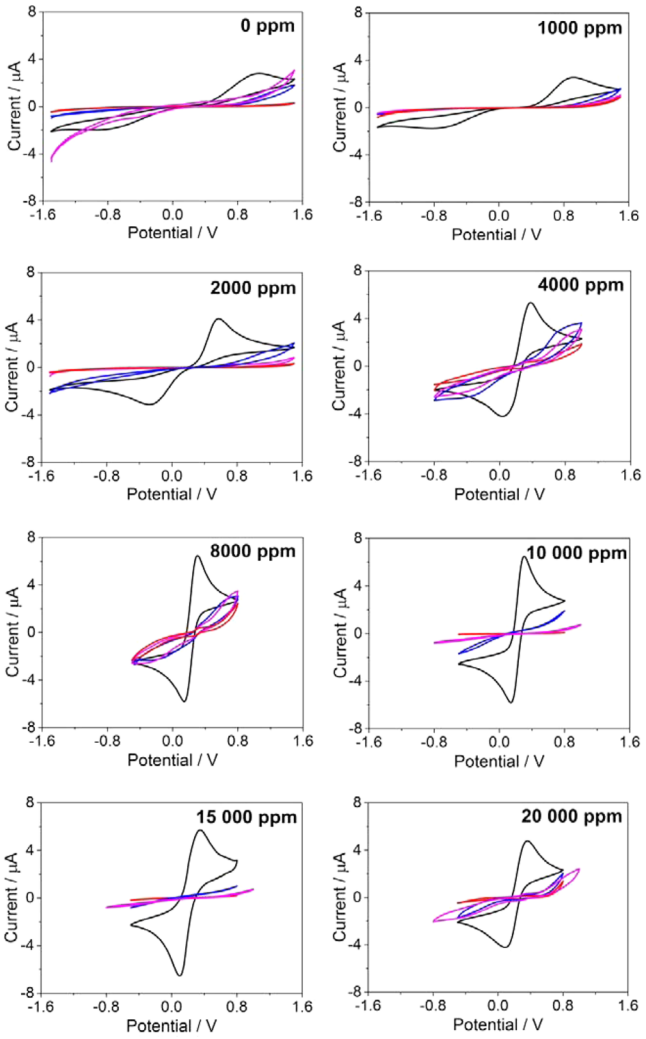

Figure 2. Cyclic voltammograms for BDD electrodes with various boron doping levels (0–20 000 ppm) before and after surface functionalization recorded in 5 mM $[Fe(CN)_6]^{3-/4-}$ containing 0.1 M KCl at a scan rate of 100 mV/s. Electrodes: bare BDD (black line), NO_2-modified BDD (red line), NH_2-modified BDD (blue line), and COOH-modified BDD (purple line).

After electrochemical grafting (red lines in Figure 2), a rapid decay of the peak currents appears, indicating a strong suppression of the electron transfer of the redox couple. This confirms the successful grafting of 4-nitrophenyl functionalities, creating an efficient barrier to the $[Fe(CN)_6]^{3-/4-}$ redox couple from approaching the BDD electrode surface.

3.3. Electrochemical and Chemical Derivatization of Grafted Functionalities. The BDD surface-tethered 4-nitrophenyl functionalities were converted to 4-aminophenyl groups by electrochemical reduction using CV in 0.1 M KCl. Nitro groups are known to be irreversibly reduced in aqueous solutions by four and/or six electrons to the corresponding hydroxylamine or amino groups, respectively.[2,9,25] Broad cathodic peaks in the first scan with different peak potentials and currents are observed for all BDD electrodes, representing the electrochemical reduction of 4-nitrophenyl to 4-aminophenyl (Figure S5). The reduction currents without any distinct peak potentials are likely related to the combined contribution from the reduction of nitro groups and hydrogen evolution. The peak currents of highly doped BDD surfaces are higher compared to those with a low doping level. This is in accordance with the previously mentioned smaller charge consumed during the electrochemical conversion of 4-nitrophenyl to 4-aminophenyl groups and the charge for grafting of the 4-nitrophenyl diazonium cations for lower boron levels. Moreover, the reduction peaks decrease during subsequent scans and anodic and cathodic peaks centered around −0.2 V appear which are attributed to the aminohydroxyphenyl/nitrosophenyl couple, indicating that 4-nitrophenyl groups at the BDD surfaces are transformed to 4-aminophenyl groups.

Electrochemical blocking properties of the 4-amino terminated grafted layer were also characterized by CV in 5 mM $[Fe(CN)_6]^{3-/4-}$ in 0.1 M KCl. The 4-aminophenyl moieties provide a slightly different blocking efficiency compared to the 4-nitrophenyl terminated surface. Figure 2 shows a slight improvement of the electron transfer for 4-aminophenyl modified BDD electrodes (blue lines) as compared to 4-nitrophenyl modified BDD electrodes. This is supposed to be due to different electrostatic interactions in these two cases. The 4-aminophenyl modified BDD surface remains moderately protonated, while the 4-nitrophenyl modified BDD surface possesses a partially negative charge from its resonance structure. This results in an electrostatic attraction or repulsion, respectively, between the charged BDD surfaces and the redox couple.

The reaction with succinic acid in the presence of the activator CDI leads to the formation of amide bonds with terminated (mostly activated) carboxyl groups at the surface. The carboxylic moieties exert an electrostatic repulsion for the redox probe which hampers its diffusion to the electrode surface.

3.4. DNA Hybridization Assay. DNA hybridization efficiency depends greatly on the coverage of the DNA probe.[35] Therefore, several strategies to control and predefine the amount of the DNA probe at the electrode surface exist, e.g., by controlling the DNA concentration, ionic strength of the solution, duration of the immobilization, or dilution of the DNA by other molecules.[36] Here, we show that the DNA coverage can be efficiently controlled by varying the boron doping level of diamond electrodes.

After modification with succinic acid, we obtained at least partially CDI-activated carboxyl groups at the surface which serve as active sites for the subsequent covalent immobilization of amino-terminated ssDNA probes. The relative amount, i.e., surface coverage of activated carboxyl-groups at the BDD electrode surface is influenced by the grafting process and hence supposed to vary with the boron doping. DNA target molecules were modified with Fc labels, allowing the detection of the hybridization process by DPV. The Fc moieties were placed on the 5′ end of the target strand, assuring the closest possible proximity to the electrode and fast electron transfer.

Figure 3 shows the DPVs for the hybridization assay at a DNA probe carboxyl-modified BDD electrode (S1/COOH-BDD) as a function of different boron doping levels. Since the amount of tethered 4-nitrophenyl functionalities at the surface increases with the boron doping level, the amount of free carboxylic groups and therefore ssDNA strands increases as well.

At low DNA probe coverage, electrostatic repulsion between neighboring DNA strands is minimal, and therefore the hybridization efficiency is maximum (Scheme 2A). However, the Fc oxidation signal is then limited by the low amount of DNA at the surface. With increasing DNA probe coverage, the

DOI: 10.1021/acsami.5b06394
ACS Appl. Mater. Interfaces 2015, 7, 18949–18956

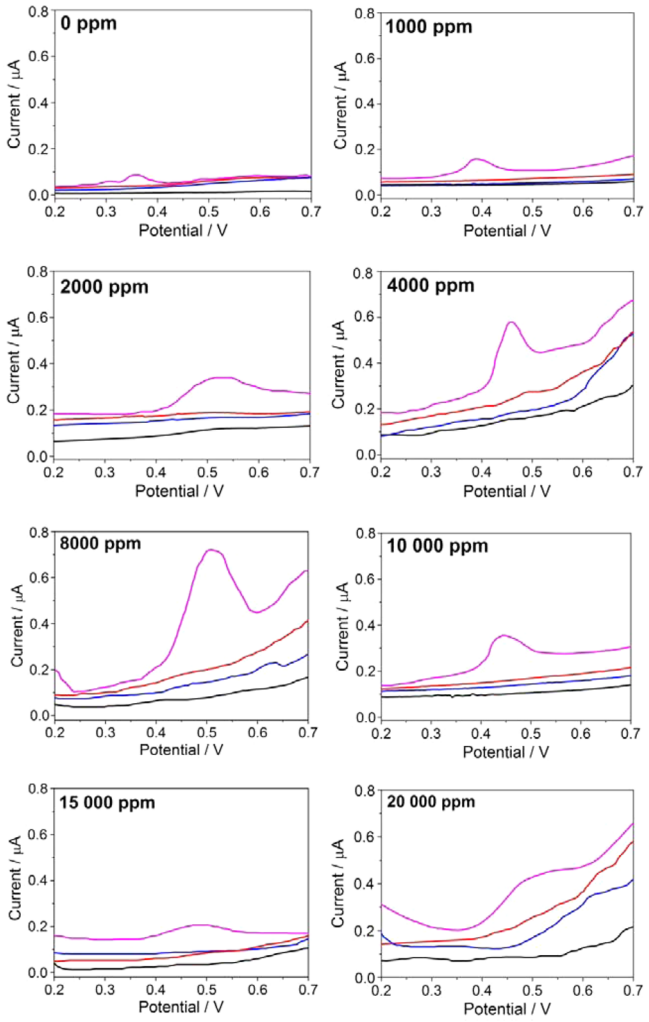

Figure 3. Differential pulse voltammograms for BDD electrodes with various boron doping levels (0−20 000 ppm) in PB with K_2SO_4 (pH 7.4). Electrodes: COOH-BDD (black line), S1/COOH-BDD (blue line), S2/COOH-BDD (red line), and S1−S2/COOH-BDD (purple line). S1 = NH_2-functionalized DNA, S2 = ferrocene labeled DNA.

hybridization yield and therefore the Fc signal, increases as well (Scheme 2A). This is observed for boron levels of up to 8000 ppm (S2/COOH-BDD in Figure 3). However, for BDD electrodes with a higher doping level, the probe DNA coverage and by this the charge density at the surface becomes too high, leading to a significant decrease in the hybridization efficiency and the hybridization yield (Scheme 2C)[37,38] as observed for electrodes with boron levels higher than 8000 ppm (Figure 4).

In order to confirm that the detected Fc signal is only due to the hybridization process, we investigated nonspecific adsorption of the target DNA. Figure 3 demonstrates that unspecific adsorption of the target to carboxyl-modified BDD does not occur regardless of the boron doping level.

Moreover, as mentioned previously, the sp^2/sp^3 carbon ratio increases from about 1.5% for the BDD electrode with boron level of 0 ppm to 4% for the 20 000 ppm. This difference cannot provide a significant increase in diamond film conductivity (ultrananocrystalline diamond films with 8% of sp^2 are several orders less conductive). Hence, the increase of the sp^2/sp^3 carbon ratio cannot be the main reason for the increased current signal after hybridization. This is further supported by the fact that for the BDD electrodes with a boron

Scheme 2. Dependence of the Hybridization Yield on the Boron Doping Level[a]

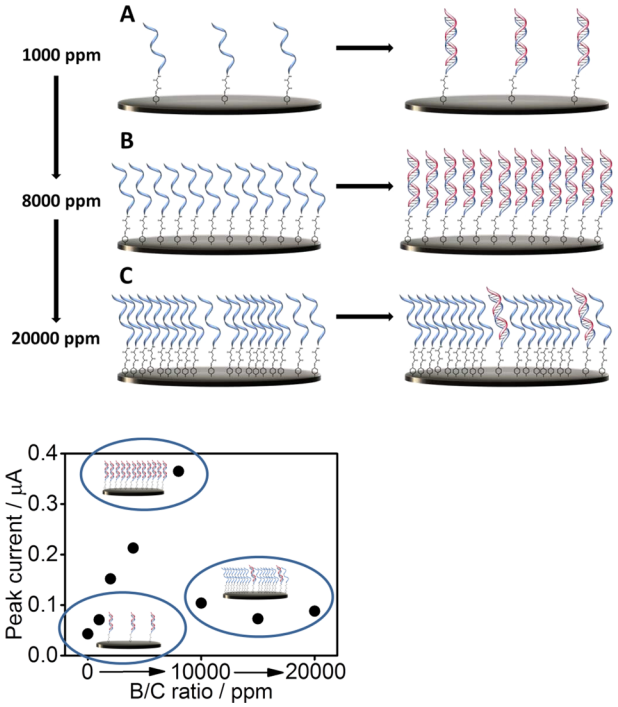

[a](A) Low boron doping levels lead to low DNA probe coverage; (B) an optimum of boron doping level and DNA probe coverage yields the highest hybridization signal; and (C) high boron doping levels leading to crowding on DNA modified surfaces resulting in poor hybridization efficiency.

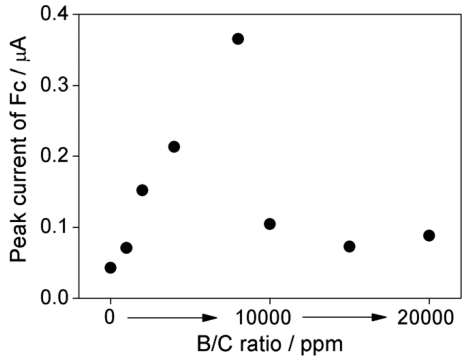

Figure 4. Hybridization yield in dependence of the boron doping level.

level higher than 8000 ppm, the current signal after DNA hybridization decreases despite the further increase in the sp^2 amount. Similarly, although the conductivity and the grain size may slightly influence the current signal, these phenomena cannot be correlated with the maximum of the signal current obtained for the BDD electrode with boron level of 8000 ppm. Taking all this into account, it can be concluded that the current signal recorded upon hybridization of modified BDD electrodes is unequivocally related to the boron doping level and with this to the DNA probe coverage.

4. CONCLUSIONS

A novel strategy for the control of surface functionalization of boron-doped diamond electrodes based on the investigation of the effect of boron doping levels on the electrochemical grafting

DOI: 10.1021/acsami.5b06394
ACS Appl. Mater. Interfaces 2015, 7, 18949−18956

of aryldiazonium salt was established. It was shown that the grafting efficiency increases with increasing boron doping level, which was assumed due to the increase of the specific conductivity. Amino functionalities introduced by grafting of nitro groups and subsequent electrochemical reduction were used to control the coverage of immobilized DNA probes at the surface. We observed a dependence of the hybridization yield on the boron doping level. Increase of the target DNA signal was observed as the boron doping level increased to 8000 ppm. Using electrodes with a boron doping level higher than 8000 ppm, the hybridization yield decreased, presumably due to an enhanced charge density and electrostatic barrier at DNA probe modified BDD surfaces, which led consequently to a decrease of the hybridization yield. Our approach ensures highly stable surface modification typical of covalent grafting on intrinsically inert diamond surfaces but also allows fine-tuning of the surface properties. Taking the results achieved in this study into consideration, the proposed protocol paves new ways to diamond-based biosensors.

■ ASSOCIATED CONTENT

Supporting Information

The Supporting Information is available free of charge on the ACS Publications website at DOI: 10.1021/acsami.5b06394.

SEM micrographs, Raman spectra, and selected properties of the BDD films including boron concentrations determined by Raman spectroscopy, NDP, SIMS, and Hall methods, synthesis of 4-nitrophenyldiazonium tetrafluoroborate and CVs for the electrochemical reduction of 4-nitrophenyl to 4-aminophenyl groups (PDF)

■ AUTHOR INFORMATION

Corresponding Author

*E-mail: wolfgang.schuhmann@rub.de (W.S.).

Author Contributions

The manuscript was written through contributions of all authors. All authors have given approval to the final version of the manuscript.

Notes

The authors declare no competing financial interest.

■ ACKNOWLEDGMENTS

This work was supported by the Grant Agency of the Slovak Republic (Grant Nos. 1/0051/13 and 1/0361/14) and the Slovak Research and Development Agency under the Contracts No. APVV-0797-11 and APVV-0365-12. Ľ.Š. acknowledges financial support by the German Academic Exchange Service (DAAD) for supporting his research stay in Bochum.

■ ABBREVIATIONS

BDD, boron-doped diamond; CDI, 1,1′-carbonyldiimidazole; CV, cyclic voltammetry; HF CVD, hot filament chemical vapor deposition; DPV, differential pulse voltammetry; NDP, neutron depth profiling; SIMS, secondary ion mass spectrometry; SEM, scanning electron microscopy

■ REFERENCES

(1) Clausmeyer, J.; Schuhmann, W.; Plumeré, N. Electrochemical Patterning as a Tool for Fabricating Biomolecule Microarrays. *TrAC, Trends Anal. Chem.* **2014**, *58*, 23−30.

(2) Wang, J.; Firestone, M. A.; Auciello, O.; Carlisle, J. A. Surface Functionalization of Ultrananocrystalline Diamond Films by Electrochemical Reduction of Aryldiazonium Salts. *Langmuir* **2004**, *20*, 11450−11456.

(3) Bae, K. H.; Lee, K.; Kim, C.; Park, T. G. Surface Functionalized Hollow Manganese Oxide Nanoparticles for Cancer Targeted siRNA Delivery and Magnetic Resonance Imaging. *Biomaterials* **2011**, *32*, 176−184.

(4) Lin, Z.; Liu, Y.; Wong, C. Facile Fabrication of Superhydrophobic Octadecylamine-Functionalized Graphite Oxide Film. *Langmuir* **2010**, *26*, 16110−16114.

(5) Stratmann, L.; Gebala, M.; Schuhmann, W. A Chemical Lift-Off Process: Removing Non-Specific Adsorption in an Electrochemical Epstein-Barr Virus Immunoassay. *ChemPhysChem* **2013**, *14*, 2198−2207.

(6) Gebala, M.; Schuhmann, W. Understanding Properties of Electrified Interfaces as a Prerequisite for Label-Free DNA Hybridization Detection. *Phys. Chem. Chem. Phys.* **2012**, *14*, 14933−14942.

(7) Tian, H.; Tang, Z.; Zhuang, X.; Chen, X.; Jing, X. Biodegradable Synthetic Polymers: Preparation, Functionalization and Biomedical Application. *Prog. Polym. Sci.* **2012**, *37*, 237−280.

(8) Thissen, P.; Seitz, O.; Chabal, Y. J. Wet Chemical Surface Functionalization of Oxide-Free Silicon. *Prog. Surf. Sci.* **2012**, *87*, 272−290.

(9) Wang, J.; Carlisle, J. A. Covalent Immobilization of Glucose Oxidase on Conducting Ultrananocrystalline Diamond Thin Films. *Diamond Relat. Mater.* **2006**, *15*, 279−284.

(10) Szunerits, S.; Nebel, C. E.; Hamers, R. J. Surface Functionalization and Biological Applications of CVD Diamond. *MRS Bull.* **2014**, *39*, 517−524.

(11) Švorc, Ľ.; Kalcher, K. Modification-free electrochemical approach for sensitive monitoring of purine DNA bases: Simultaneous Determination of Guanine and Adenine in Biological Samples Using Boron-Doped Diamond Electrode. *Sens. Actuators, B* **2014**, *194*, 332−342.

(12) Pecková, K.; Musilová, J.; Barek, J. Boron-Doped Diamond Film Electrodes-New Tool for Voltammetric Determination of Organic Substances. *Crit. Rev. Anal. Chem.* **2009**, *39*, 148−172.

(13) Qiu, F.; Compton, R. G.; Marken, F.; Wilkins, S. J.; Goeting, C. H.; Foord, J. S. Laser Activation Voltammetry: Selective Removal of Reduced Forms of Methyl Viologen Deposited on Glassy Carbon and Boron-Doped Diamond Electrodes. *Anal. Chem.* **2000**, *72*, 2362−2370.

(14) Actis, P.; Manesse, M.; Nunes-Kirchner, C.; Wittstock, G.; Coffinier, Y.; Boukherroub, R.; Szunerits, S. Localized Electropolymerization on Oxidized Boron-Doped Diamond Electrodes Modified with Pyrrolyl Units. *Phys. Chem. Chem. Phys.* **2006**, *8*, 4924−4931.

(15) Strother, T.; Knickerbocker, T.; Russell, J. N.; Butler, J. E.; Smith, L. M.; Hamers, R. J. Photochemical Functionalization of Diamond Films. *Langmuir* **2002**, *18*, 968−971.

(16) Meziane, D.; Barras, A.; Kromka, A.; Houdkova, J.; Boukherroub, R.; Szunerits, S. Thiol-yne Reaction on Boron-Doped Diamond Electrodes: Application for the Electrochemical Detection of DNA - DNA Hybridization Events. *Anal. Chem.* **2012**, *84*, 194−200.

(17) Pinson, J.; Podvorica, F. Attachment of Organic Layers to Conductive or Semiconductive Surfaces by Reduction of Diazonium Salts. *Chem. Soc. Rev.* **2005**, *34*, 429−439.

(18) Mahouche-Chergui, S.; Gam-Derouich, S.; Mangeneya, C.; Chehimi, M. M. Aryl Diazonium Salts: a New Class of Coupling Agents for Bonding Polymers, Biomacromolecules and Nanoparticles to Surfaces. *Chem. Soc. Rev.* **2011**, *40*, 4143−4166.

(19) Griveau, S.; Mercier, D.; Vautrin-Ul, C.; Chausse, A. Electrochemical Grafting by Reduction of 4-Aminoethylbenzenediazonium Salt: Application to the Immobilization of (Bio)molecules. *Electrochem. Commun.* **2007**, *9*, 2768−2773.

(20) Allongue, P.; Delamar, M.; Desbat, B.; Fagebaume, O.; Hitmi, R.; Pinson, J.; Savéant, J. M. Covalent Modification of Carbon Surfaces

DOI: 10.1021/acsami.5b06394
ACS Appl. Mater. Interfaces 2015, 7, 18949−18956

by Aryl Radicals Generated from the Electrochemical Reduction of Diazonium Salts. *J. Am. Chem. Soc.* **1997**, *119*, 201−207.
(21) Zhou, Y. L.; Zhi, J. F. Development of an Amperometric Biosensor Based on Covalent Immobilization of Tyrosinase on a Boron-Doped Diamond Electrode. *Electrochem. Commun.* **2006**, *8*, 1811−1816.
(22) Härtl, A.; Schmich, E.; Garrido, J. A.; Hernando, J.; Catharino, S. C. R.; Walter, S.; Feulner, P.; Kromka, A.; Steinmüller, D.; Stutzmann, M. Protein-Modified Nanocrystalline Diamond Thin Films for Biosensor Applications. *Nat. Mater.* **2004**, *3*, 736−742.
(23) Agnès, C.; Arnault, J. C.; Omnès, F.; Jousselme, B.; Billon, M.; Bidand, G.; Mailley, P. XPS Study of Ruthenium Tris-Bipyridine Electrografted from Diazonium Salt Derivative on Microcrystalline Boron Doped Diamond. *Phys. Chem. Chem. Phys.* **2009**, *11*, 11647−11654.
(24) Rezek, B.; Shin, D.; Nebel, C. E. Properties of Hybridized DNA Arrays on Single-Crystalline Undoped and Boron-Doped (100) Diamonds Studied by Atomic Force Microscopy in Electrolytes. *Langmuir* **2007**, *23*, 7626−7633.
(25) Uetsuka, H.; Shin, D.; Tokuda, N.; Saeki, K.; Nebel, C. E. Electrochemical Grafting of Boron-Doped Single-Crystalline Chemical Vapor Deposition Diamond with Nitrophenyl Molecules. *Langmuir* **2007**, *23*, 3466−3472.
(26) Yang, N.; Yu, J.; Uetsuka, H.; Nebel, C. E. Characterization of Diamond Surface Terminations Using Electrochemical Grafting with Diazonium Salts. *Electrochem. Commun.* **2009**, *11*, 2237−2240.
(27) Shul, G.; Actis, P.; Marcus, B.; Opallo, M.; Boukherroub, R.; Szunerits, S. Solvent-Free Chemical Functionalization of Hydrogen-Terminated Boron-Doped Diamond Electrodes with Diazonium Salts in Ionic Liquids. *Diamond Relat. Mater.* **2008**, *17*, 1394−1398.
(28) Kinder, R.; Mikolášek, M.; Donoval, D.; Kováč, J.; Tlaczala, M. Measurement System with Hall and a Four Point Probes for Characterization of Semiconductors. *J. Electr. Eng.* **2013**, *64*, 106−111.
(29) Malcher, V.; Mrška, A.; Kromka, A.; Šatka, A.; Janík, A. Diamond Film Coated on WC/Co Tools by Double Bias-Assisted Hot Filament CVD. *Curr. Appl. Phys.* **2002**, *2*, 201−204.
(30) Bernard, M.; Baron, C.; Deneuville, A. About the Origin of the Low Wave Number Structures of the Raman Spectra of Heavily Boron Doped Diamond Films. *Diamond Relat. Mater.* **2004**, *13*, 896−899.
(31) May, P. W.; Ludlow, W. J.; Hannaway, M.; Heard, P. J.; Smith, J. A.; Rosser, K. N. Raman and Conductivity Studies of Boron-Doped Microcrystalline Diamond, Facetted Nanocrystalline Diamond and Cauliflower Diamond Films. *Diamond Relat. Mater.* **2008**, *17*, 105−117.
(32) Ghodbane, S.; Deneuville, A. Specific Features of 325 nm Raman Excitation of Heavily Boron Doped Polycrystalline Diamond Films. *Diamond Relat. Mater.* **2006**, *15*, 589−592.
(33) Ballutaud, D.; Jomard, F.; Kociniewski, T.; Rzepka, E.; Girard, H.; Saada, S. Sp^3/sp^2 Character of the Carbon and Hydrogen Configuration in Micro- and Nanocrystalline Diamond. *Diamond Relat. Mater.* **2008**, *17*, 451−456.
(34) Holt, K. B.; Bard, A. J. Scanning Electrochemical Microscopy and Conductive Probe Atomic Force Microscopy Studies of Hydrogen-Terminated Boron-Doped Diamond Electrodes with Different Doping Levels. *J. Phys. Chem. B* **2004**, *108*, 15117−15127.
(35) Peterson, A. W.; Heaton, R. J.; Georgiadis, R. M. The Effect of Surface Probe Density on DNA Hybridization. *Nucleic Acids Res.* **2001**, *29*, 5163−5168.
(36) Doneux, T.; De Rache, A.; Triffaux, E.; Meunier, A.; Steichen, M.; Buess-Herman, C. Optimization of the Probe Coverage in DNA Biosensors by a One-Step Coadsorption Procedure. *ChemElectroChem* **2014**, *1*, 147−157.
(37) Gong, P.; Levicky, R. DNA Surface Hybridization Regimes. *Proc. Natl. Acad. Sci. U. S. A.* **2008**, *105*, 5301−5306.
(38) Tymoczko, J.; Schuhmann, W.; Gebala, M. Electrical Potential-Assisted DNA Hybridization. How to Mitigate Electrostatics for Surface DNA Hybridization. *ACS Appl. Mater. Interfaces* **2014**, *6*, 21851−21858.

DOI: 10.1021/acsami.5b06394
ACS Appl. Mater. Interfaces 2015, 7, 18949−18956